

# Precise Computation of Drag Coefficients of the Sphere <sup>1</sup>

Masahisa Tabata (田端正久)  
Kazuhiro Itakura (板倉和宏)

Department of Mathematics, Hiroshima University  
Higashi-Hiroshima, 739 Japan

## 1. Introduction

The computation of the drag coefficient of a body immersed in a fluid is the subject which attracts many researchers, e.g., see [1], [2], [3], [4], [5] and their references. It has not only the practical importance such as the case of aircrafts or cars, but also it is a good bench mark problem for new flow codes. To the best of our knowledge, however, there are no literatures discussing the preciseness of drag coefficients by using an error estimate even in the case of the circular cylinder or the sphere.

In this paper we present precise computation of drag coefficients of the sphere by using two finite element schemes for axisymmetric flow problems developed by ourselves recently [6],[7]. One is an extension of the standard mixed finite element method to axisymmetric problems, and the other is an extension of the stabilized finite element method. Our method of computing drag coefficients may be considered as a consistent flux method [8], [9], [10], but we fix a proper test function, which enables us to obtain error estimates of drag coefficients under some assumption. Moreover our numerical results show that P2/P1 mixed finite element scheme produces lower bounds and that P1/P1 stabilized finite element scheme does upper bounds. Combining these facts and an extrapolation of numerical results, we obtain drag coefficients of the sphere for the Reynolds numbers between 10 and 200.

## 2. Drag coefficients of axisymmetric bodies

Let  $G$  be a body in a velocity field. Let  $U$  be the representative velocity and  $\rho$  be the density of the fluid. The drag coefficient of  $G$  is defined by

$$C_D = \frac{D}{\frac{1}{2}\rho U^2 A},$$

where  $D$  is the total force exerted on  $G$  by the fluid and  $A$  is the area of cross section of  $G$  to the direction  $U$ .

When the direction of  $U$  coincides with the z-axis, the drag coefficient is written as

$$C_D = -\frac{2}{\rho U^2 A} \int_S (\sigma_{zx} n_x + \sigma_{zy} n_y + \sigma_{zz} n_z) dS,$$

---

<sup>1</sup>In this paper all proofs are omitted. They are found in the paper submitted to Computational Methods in Applied Mechanics and Engineering by the same authors.

where  $\sigma$  is the stress tensor,  $S$  is the surface of  $G$ , and  $n = (n_x, n_y, n_z)^T$  is the unit outer normal (from the fluid) to  $S$ .

Suppose that  $G$  is axisymmetric with respect to  $z$ -axis. We introduce the cylindrical coordinates  $(x_1, \theta, x_2)$ , where  $x_1$  is the distance from  $z$ -axis and  $x_2$  is equal to  $z$ . Furthermore we assume the flow is axisymmetric, i.e.,

$$u_1 = u_1(x_1, x_2), \quad u_\theta = 0, \quad u_2 = u_2(x_1, x_2), \quad p = p(x_1, x_2),$$

where  $(u_1, u_\theta, u_2)^T$  is the velocity and  $p$  is the pressure. Then the three-dimensional problem can be reduced to a two-dimensional problem in a meridian. Let  $C$  be an intersection curve of  $S$  and the meridian ( $x_1 > 0$ ). Then the drag coefficient is rewritten as

$$C_D = -\frac{4\pi}{\rho U^2 A} \int_C \sum_{j=1}^2 \sigma_{2j}(u, p) n_j x_1 ds, \quad (1)$$

where  $\sigma$  is the stress tensor defined by

$$\sigma_{ij}(u, p) = -p\delta_{ij} + \frac{2}{Re} D_{ij}(u), \quad D_{ij}(u) = \frac{1}{2} \left( \frac{\partial u_i}{\partial x_j} + \frac{\partial u_j}{\partial x_i} \right) \quad (2)$$

and  $n = (n_1, n_2)^T$  is the unit outer normal (from the fluid) to  $C$ .

Here we briefly review the finite element formulation for axisymmetric flows [6],[7]. Let  $\Omega$  be a meridian of an axisymmetric domain in  $\mathbf{R}^3$ . We denote the point in  $\Omega$  by  $x = (x_1, x_2)$  as above. The stationary axisymmetric Navier-Stokes equations are written as

$$(u \cdot \text{grad})u + \frac{1}{Re} Lu + \text{grad } p = f \quad (x \in \Omega), \quad (3)$$

$$\text{div}_1 u = 0 \quad (x \in \Omega), \quad (4)$$

where  $u = (u_1, u_2)^T$  is the velocity,  $p$  is the pressure,  $f = (f_1, f_2)^T$  is an external force,  $Re$  is the Reynolds number, and

$$\text{div}_1 u = \frac{1}{x_1} \text{div}(x_1 u), \quad \Delta_1 = \frac{\partial^2}{\partial x_1^2} + \frac{1}{x_1} \frac{\partial}{\partial x_1} + \frac{\partial^2}{\partial x_2^2},$$

$$L = \begin{bmatrix} -\Delta_1 + \frac{1}{x_1^2} & 0 \\ 0 & -\Delta_1 \end{bmatrix}.$$

We note that the differential operators acting each component of the velocity are different and that they have singularities on the axis  $x_1 = 0$ . Considering these facts, we introduce function spaces [6],[11],

$$X_{1/2}^{\ell,2}(\Omega) = \{v : \Omega \rightarrow \mathbf{R}; x_1^{\frac{1}{2}-\ell+|\beta|} D^\beta v \in L^2(\Omega), 0 \leq |\beta| \leq \ell\},$$

$$W_{1/2}^{\ell,2}(\Omega) = \{v : \Omega \rightarrow \mathbf{R}; x_1^{\frac{1}{2}} D^\beta v \in L^2(\Omega), 0 \leq |\beta| \leq \ell\}.$$

The velocity  $u$  and the pressure  $p$  are sought in

$$u_1 \in X_{1/2}^{1,2}(\Omega), \quad u_2 \in W_{1/2}^{1,2}(\Omega), \quad p \in L_{1/2}^2(\Omega) (\equiv W_{1/2}^{0,2}(\Omega)).$$

We define a trilinear form  $a_1$  and two bilinear forms  $a$  and  $b$  by

$$\begin{aligned} a_1(w, u, v) &= \int_{\Omega} \sum_{j=1}^2 (w \cdot \text{grad} u_j) v_j x_1 dx, \\ a(u, v) &= \frac{2}{Re} \int_{\Omega} \left\{ \sum_{i,j=1}^2 D_{ij}(u) D_{ij}(v) + \frac{u_1 v_1}{x_1^2} \right\} x_1 dx, \\ b(v, q) &= - \int_{\Omega} q \text{div}_1 v x_1 dx. \end{aligned}$$

The following proposition is proved easily by using the Gauss-Green theorem.

**Proposition 1.** *Let  $(u_1, u_2, p)$  be any functions in  $X_{1/2}^{2,2}(\Omega) \times W_{1/2}^{2,2}(\Omega) \times W_{1/2}^{1,2}(\Omega)$ . Then for any function  $v \in X_{1/2}^{1,2}(\Omega) \times W_{1/2}^{1,2}(\Omega)$  we have*

$$\begin{aligned} & a_1(u, u, v) + a(u, v) + b(v, p) \\ &= \int_{\Omega} \left\{ (u \cdot \text{grad})u + \frac{1}{Re} Lu + \text{grad}p + \frac{1}{Re} \text{grad}(\text{div}_1 u) \right\} v x_1 dx \\ & \quad + \int_{\partial\Omega} [\sigma(u, p)] n v x_1 ds, \end{aligned}$$

where  $\sigma(u, p)$  is the stress tensor defined by (2).

Suppose  $f$  is given in  $(L_{1/2}^2(\Omega))^2$ . Let  $(u, p)$  be a solution of (3) and (4) subject to a boundary condition. If  $(u, p)$  has the regularity assumed in Proposition 1, we have

$$\int_{\partial\Omega} [\sigma(u, p)] n v x_1 ds = a_1(u, u, v) + a(u, v) + b(v, p) - \langle f, v \rangle, \quad (5)$$

for any function  $v \in X_{1/2}^{1,2}(\Omega) \times W_{1/2}^{1,2}(\Omega)$ , where

$$\langle f, v \rangle = \int_{\Omega} f \cdot v x_1 dx.$$

Since (5) is meaningful for the function  $(u_1, u_2, p) \in X_{1/2}^{1,2}(\Omega) \times W_{1/2}^{1,2}(\Omega) \times L_{1/2}^2(\Omega)$ , (5) is valid for the (weak) solution  $(u, p)$  of (3) and (4). Let  $C$  be the intersection curve mentioned above.  $C$  is a portion of the boundary  $\partial\Omega$ . Let  $v^* = (0, v_2^*)$  be a fixed function such that

$$v_2^* \in W_{1/2}^{1,2}(\Omega), \quad v_2^* = 1 \quad \text{on } C, \quad v_2^* x_1 \sum_{j=1}^2 \sigma_{2j}(u, p) n_j = 0 \quad \text{on } \partial\Omega \setminus C. \quad (6)$$

From (1) and (5) we obtain

$$C_D = - \frac{4\pi}{\rho U^2 A} \{ a_1(u, u, v^*) + a(u, v^*) + b(v^*, p) - \langle f, v^* \rangle \}. \quad (7)$$

We employ (7) for the computation of the drag coefficient.

Let  $(u_{1h}, u_{2h}, p_h) \in X_{1/2}^{1,2}(\Omega) \times W_{1/2}^{1,2}(\Omega) \times L_{1/2}^2(\Omega)$  be a corresponding finite element

solution. Let  $v_h^*$  be an interpolation of  $v^*$  in the finite element space. We define an approximate drag coefficient  $C_D^h$  by

$$C_D^h = -\frac{4\pi}{\rho U^2 A} \{a_1(u_h, u_h, v_h^*) + a(u_h, v_h^*) + b(v_h^*, p_h) - \langle f, v_h^* \rangle\}. \quad (8)$$

**Remark 1.** (i) We have derived (8) for axisymmetric flow problems in the cylindrical coordinates. The corresponding result (including the computation of lift coefficients) for the general flow problems in the Cartesian coordinates can be obtained similarly.

(ii) The drag coefficient  $C_D^h$  applied to the problem in the Cartesian coordinates coincides with that obtained from the consistent flux method [8],[9],[10]. In those papers, however, the function  $v^*$  is not used. As will be shown soon the use of  $v^*$  enables us to derive an error estimate.

(iii) The direct boundary integration (1) for finite element solutions produces poor results (see Section 4). Similar facts are pointed out also in the literatures cited just above. In (1) the boundary values of  $gradu$  and  $p$  appear. In general, the estimate at the boundary of a function is harder than that in the interior (we need more regularity). That is the reason why we employ (8) for the computation of drag coefficients, where only interior integrals appear and there are no boundary terms.

(iv) In the real computation of  $C_D^h$  we replace the function  $v_h^*$  by a more convenient function, which makes the computation simpler but does not change the value (see Theorem 2).

**Proposition 2.** *There exists a positive constant*

$$c_1 = c_1(\|u\|_V, \|u_h\|_V, \|v^*\|_V, \|f\|_{(L^2_{1/2}(\Omega))^2}, \rho, U, A, Re)$$

such that

$$|C_D - C_D^h| \leq c_1 \{ \|u - u_h\|_V + \|p - p_h\|_Q + \|v^* - v_h^*\|_V \}, \quad (9)$$

where  $V$ -norm and  $Q$ -norm represent the  $X^1_{1/2}(\Omega) \times W^1_{1/2}(\Omega)$  norm and the  $L^2_{1/2}(\Omega)$  norm, respectively.

Let  $h$  be a discretization parameter of the domain, i.e., the maximum diameter of elements.

**Theorem 1.** *Suppose that there exist positive constants  $c_2$  and  $\alpha$  independent of  $h$  such that*

$$\|u - u_h\|_V, \|p - p_h\|_Q, \|v^* - v_h^*\|_V \leq c_2 h^\alpha. \quad (10)$$

Then we have

$$|C_D - C_D^h| \leq c_3 h^\alpha, \quad (11)$$

where  $c_3$  is a positive constant independent of  $h$ .

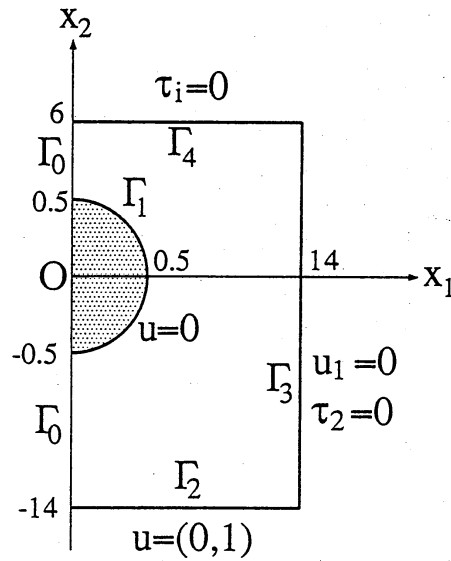


Figure 1: Statement of the problem

### 3. Computation of drag coefficients of the sphere

Here we compute drag coefficients of the sphere. We consider a domain  $\Omega$  shown in Fig. 1. At the origin there exists a sphere of unit diameter. We note that the scale of Fig.1 is distorted. For the figure scaled correctly we refer to Fig. 2.

The equations we consider are (3) and (4), where  $f = 0$ . The boundary conditions are shown in Fig. 1, where  $\tau$  is the stress vector defined by

$$\tau(u, p) = [\sigma(u, p)]n.$$

Let  $g$  be a given velocity on  $\Gamma_2$ . We define an affine space  $V(g)$  by

$$V(g) = \{v = (v_1, v_2) \in X_{1/2}^{1,2}(\Omega) \times W_{1/2}^{1,2}(\Omega); v = 0 \text{ on } \Gamma_1, v = g \text{ on } \Gamma_2, v_1 = 0 \text{ on } \Gamma_3\}.$$

We denote  $V(0)$  by  $V$ .

We seek the velocity  $u$  in  $V((0, 1))$  and the pressure  $p$  in  $Q \equiv L_{1/2}^2(\Omega)$ . Then the variational formulation of our problem is :

$$a_1(u, u, v) + a(u, v) + b(v, p) = 0 \quad (\forall v \in V), \quad (12)$$

$$b(u, q) = 0 \quad (\forall q \in Q). \quad (13)$$

In our problem  $C = \Gamma_1$ . We choose a function  $v^*$  satisfying (6). For example,  $v^* = (0, v_2^*)$ , where  $v_2^* \in C^\infty(\bar{\Omega})$  and

$$v_2^*(x_2) = \begin{cases} 1 & (x_2 \geq -0.5), \\ 0 & (x_2 = -14). \end{cases}$$

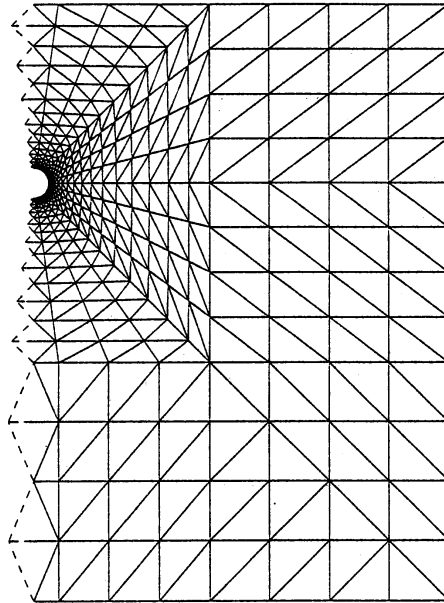


Figure 2: Subdivision of the domain (N=16)

Setting

$$\rho = 1, \quad U = 1, \quad A = \frac{\pi}{4},$$

we have

$$C_D = -16\{a_1(u, u, v^*) + a(u, v^*) + b(v^*, p)\}.$$

**Remark 2.** (i) After having studied the influence of the boundedness of the domain, we have chosen the domain shown in Fig. 1 [12]. Here we do not present the detail, but we note that our choice is suitable for low Reynolds number flows where no Kármán vortices appear.

(ii) The condition

$$u_1 = 0 \quad \text{on } \Gamma_0$$

is automatically implied from  $u_1 \in X_{1/2}^{1,2}(\Omega)$  (see [6],[11]).

Now we solve the problem (12) and (13) by two kinds of finite element schemes. We divide the domain  $\Omega$  into a union of triangles (see Fig.2). Let  $V_h$  and  $Q_h$  be finite dimensional subspaces of  $V$  and  $Q$ , respectively.

The first choice of finite elements is  $P2/P1$ . The mixed finite element formulation of (12) and (13) is: Find  $(u_h, p_h) \in V_h((0, 1)) \times Q_h$  such that

$$a_1(u_h, u_h, v_h) + a(u_h, v_h) + b(v_h, p_h) = 0 \quad (\forall v_h \in V_h), \quad (14)$$

$$b(u_h, q_h) = 0 \quad (\forall q_h \in Q_h). \quad (15)$$

The second choice of finite elements is  $P1/P1$ . In this case we use the stabilized finite element formulation: Find  $(u_h, p_h) \in V_h((0, 1)) \times Q_h$  such that

$$\mathcal{A}_h(u_h)((u_h, p_h), (v_h, q_h)) = 0 \quad (\forall (v_h, q_h) \in \mathcal{V}_h),$$

where  $\mathcal{V}_h$  is the product space

$$\mathcal{V}_h = V_h \times Q_h$$

and  $\mathcal{A}_h(u_h)$  is a bilinear form in  $\mathcal{V}_h$  defined by

$$\begin{aligned} & \mathcal{A}_h(w_h)((u_h, p_h), (v_h, q_h)) \\ &= a_1(w_h, u_h, v_h) + a(u_h, v_h) + b(v_h, p_h) + b(u_h, q_h) + \mathcal{C}_h(w_h)((u_h, p_h), (v_h, q_h)), \end{aligned}$$

$$\begin{aligned} & \mathcal{C}_h(w)((u_h, p_h), (v_h, q_h)) = \sum_K \tau_K \\ & \times \int_K \left\{ (w \cdot \text{grad})u_h + \frac{1}{Re} Lu_h + \text{grad } p_h \right\} \left\{ (w \cdot \text{grad})v_h + \frac{1}{Re} Lv_h - \text{grad } q_h \right\} x_1 dx. \end{aligned}$$

Here the summation is taken for all elements  $K$  and  $\tau_K$  is the stabilization parameter defined by

$$\tau_K = \begin{cases} h_K^2 Re / (4c_0^2) & \text{when } Re_K < 1, \\ h_K / (2|w_K|) & \text{when } Re_K \geq 1, \end{cases}$$

where  $Re_K$  is an element Reynolds number

$$Re_K = \frac{h_K |w_K| Re}{2c_0^2},$$

$h_K$  is the diameter of element  $K$ ,  $w_K$  is a representative velocity of  $w$  in  $K$ , e.g., the value of  $w$  at the centroid of  $K$ , and  $c_0$  is a positive constant independent of  $h$ .

**Remark 3.** (i) In the case of axisymmetric problems the construction of finite element subspaces is not so trivial because of the appearance of the singularity on the axis. Especially in the stabilized finite element method we have to use a symmetric decomposition with respect to the axis as shown in Fig. 2. For the details we refer to [6],[7].

(ii) For the choice of the stabilization parameter  $\tau_K$  we refer to [13],[14].

After obtaining the finite element solution  $(u_h, p_h)$  we get the drag coefficient by

$$C_D^h = -16 \{ a_1(u_h, u_h, v_h^*) + a(u_h, v_h^*) + b(v_h^*, p_h) \}, \quad (16)$$

where  $v_h^*$  is the interpolation of  $v^*$  in the finite element space.

**Theorem 2.** Let  $\phi_h = (0, \phi_{2h})$  be a function in the velocity finite element space defined by

$$\phi_{2h} = \begin{cases} 1 & \text{at all nodal points on } C, \\ 0 & \text{at the other nodal points.} \end{cases}$$

Suppose  $(u_h, p_h)$  is the solution of (14) and (15). Then we have

$$C_D^h = -16\{a_1(u_h, u_h, \phi_h) + a(u_h, \phi_h) + b(\phi_h, p_h)\}. \quad (17)$$

**Remark 4.** (i) (17) makes the computation  $C_D^h$  easier. We do not need the values of  $v^*$ , but need only some manipulations of the stiffness matrices and the finite element solution.

(ii) In the case of the stabilized finite element method we may replace (16) by

$$C_D^{hs} = -16\{a_1(u_h, u_h, v_h^*) + a(u_h, v_h^*) + b(v_h^*, p_h) + \mathcal{C}_h(u_h)((u_h, p_h), (v_h^*, 0))\}.$$

Then as Theorem 2 we can show

$$C_D^{hs} = -16\{a_1(u_h, u_h, \phi_h) + a(u_h, \phi_h) + b(\phi_h, p_h) + \mathcal{C}_h(u_h)((u_h, p_h), (\phi_h, 0))\}. \quad (18)$$

We assume the condition of Theorem 1. The exact solution  $(u, p)$  satisfies

$$\mathcal{C}_h(u)((u, p), (v_h^*, 0)) = 0.$$

Hence if there exists a positive constant  $c_4$  independent of  $h$  such that

$$|\mathcal{C}_h(u)((u, p), (v_h^*, 0)) - \mathcal{C}_h(u_h)((u_h, p_h), (v_h^*, 0))| \leq c_4 h^\alpha, \quad (19)$$

we have

$$|C_D - C_D^{hs}| \leq c_5 h^\alpha, \quad (20)$$

where  $c_5$  is a positive constant independent of  $h$ .

## 4. Numerical results of the drag coefficients

Let  $N$  be the representative subdivision number of the domain (the element size is of order  $1/N$ ). Fig. 2 shows the subdivision of  $N = 16$  for the P2/P1 element. The subdivision for the P1/P1 element is obtained by dividing each triangle into four congruent triangles (and a suitable modification is done for elements adjacent to the boundary). Total element numbers and freedoms of velocity and pressure for  $N=16,40,48$  are listed in Table 1.

At first we study the convergence of  $C_D^h$  and  $C_D^{hs}$  when  $N$  becomes large, i.e., the element size  $h$  becomes small. Fig.3 shows the behavior of drag coefficients for  $Re = 100$  when  $N$  increases. The white marks depict the values of  $C_D^h$  (P2/P1 element) and  $C_D^{hs}$  (P1/P1 element) and the black marks depict the values  $\tilde{C}_D^h$  obtained by the direct boundary integration of  $(u_h, p_h)$ ,

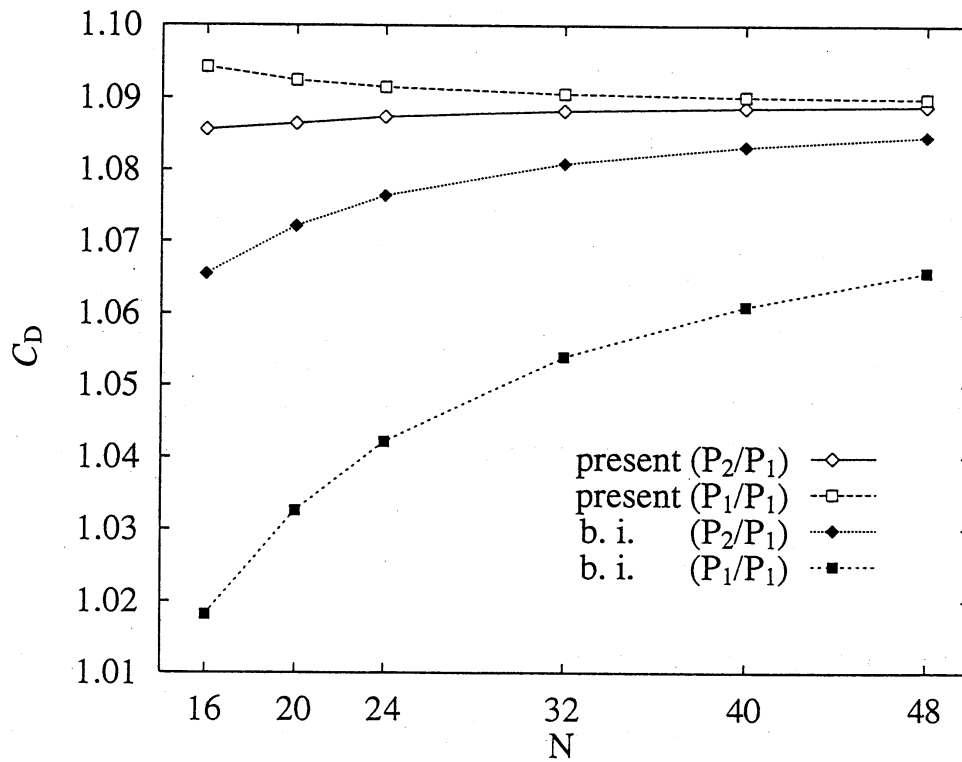
$$\tilde{C}_D^h = -16 \int_C \sum_{j=1}^2 \sigma_{2j}(u_h, p_h) n_j x_1 ds$$

for P2/P1 and P1/P1 elements. We see that the convergences of  $C_D^h$  and  $C_D^{hs}$  are much faster than  $\tilde{C}_D^h$ .



Table 1: Total element number( $N_e$ ) and freedoms of velocity( $N_u$ ) and pressure( $N_p$ )

$N$	P2/P1			P1/P1		
	$N_e$	$N_u$	$N_p$	$N_e$	$N_u$	$N_p$
16	640	2,538	323	2,560	2,574	1,287
40	4,000	15,948	2,009	16,000	16,038	8,019
48	5,760	22,978	2,891	23,040	23,086	11,543

Figure 3: Convergence of drag coefficients ( $N$  is the number of subdivision and b.i. stands for the boundary integral)

From Fig. 3 we observe that  $C_D^h$  converges from below and that  $C_D^{hs}$  converges from upper. The convergence of  $C_D^h$  is faster than that of  $C_D^{hs}$ , which is an expected result from the approximation property of the finite element spaces. In fact, the P2/P1 space has the approximation ability of

$$\|u - u_h^*\|_V, \|p - p_h^*\|_Q \sim O(h^2),$$

where  $u_h^*$  and  $p_h^*$  are interpolations. On the other hand the P1/P1 space has the approximation ability of

$$\|u - u_h^*\|_V \sim O(h), \|p - p_h^*\|_Q \sim O(h^2).$$

Hence  $\alpha$  in (11) is (at most) equal to 2 and  $\alpha$  in (20) is (at most) equal to 1.

**Remark 5.** Consider the Stokes problem or the Navier-Stokes problem with low Reynolds numbers. Then for the P2/P1 element and for the stabilized P1/P1 element (10) holds with  $\alpha=2$  and 1, respectively [7]. For the stabilized P1/P1 element we can show (19) with  $\alpha=1$  if  $|u_h|$  is bounded uniformly with respect to  $h$ .

From the above observation we assume that  $C_D^h$  is written as

$$C_D^h = C_D - \frac{c}{N^2}$$

where  $c$  is a constant independent of  $h \sim 1/N$ . By using the results of  $N=40$  and 48, we extrapolate the values  $C_D^h$ . Table 2 shows the results  $C_D$  obtained like this as well as  $C_D^h$  (P2/P1 element),  $C_D^{hs}$  (P1/P1 element), and those by Shirayama [4] and Schlichting [15]. Shirayama's results are based on finite difference computation in a three dimensional domain. Schlichting's results are based on physical experiments. We read the values from a  $Re-C_D$  graph in his book. Fig. 4 depicts the graphs of  $C_D$  and others of Table 2. Since we cannot distinguish  $C_D$ ,  $C_D^h$  and  $C_D^{hs}$  in the graph, they are marked by common circles. When  $Re$  is greater than 200, the Kármán vortex appears and the flow is no longer axisymmetric. We therefore stopped the calculation of drag coefficients at  $Re = 200$ .

## 5. Concluding remarks

We have presented a computational method of drag coefficients of axisymmetric bodies and have obtained drag coefficients of the sphere for Reynolds numbers between 10 and 200. We used two kinds of finite element schemes, P2/P1 mixed scheme and P1/P1 stabilized scheme. It has not proved yet theoretically but the numerical results have shown that the former gives lower bounds of the drag coefficients and the latter gives upper bounds.

In order to obtain drag coefficients for higher Reynolds numbers we have to solve three dimensional problems because the Kármán vortices appear. To those problems our method is also applicable not only for drag coefficients but also for lift coefficients.

The application to drag and lift coefficients of cylinders is straightforward at

Table 2: Drag coefficients of the sphere

$Re$	$C_D$	$C_D^h$	$C_D^{hs}$	Shirayama	Schlichting
10	4.3178	4.3159	4.3194	4.255	4.35
15	3.2805	3.2790	3.2817		3.34
20	2.7240	2.7227	2.7250	2.622	2.79
25	2.3700	2.3689	2.3709		2.42
30	2.1218	2.1207	2.1225	2.066	2.17
40	1.7917	1.7908	1.7924	1.741	1.84
50	1.5785	1.5777	1.5791	1.532	1.61
60	1.4272	1.4264	1.4277	1.427	1.46
70	1.3131	1.3124	1.3136	1.313	1.33
80	1.2233	1.2226	1.2238	1.222	1.23
90	1.1503	1.1497	1.1508	1.149	1.17
100	1.0895	1.0889	1.0900	1.104	1.11
125	0.97316	0.97265	0.97363		0.995
150	0.88887	0.88841	0.88933	0.901	0.918
175	0.82396	0.82353	0.82439		0.853
200	0.77176	0.77136	0.77218	0.784	0.807

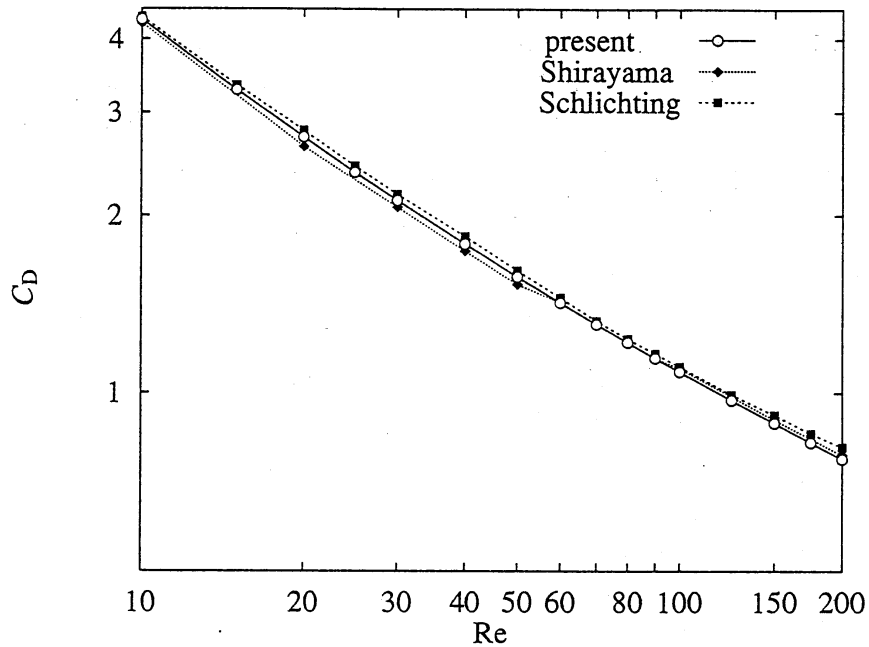


Figure 4: Drag coefficient of the sphere vs. Reynolds number

least for not so high Reynolds numbers. For high Reynolds numbers some kind of upwind techniques and fine mesh subdivisions in boundary layers as considered in [3] will be required.

## References

- [1] P. M. Gresho, S. T. Chan, R. L. Lee, and C. D. Upson. A modified finite element method for solving the time-dependent, incompressible Navier-Stokes equations, Part 2 : Applications. *International Journal for Numerical Methods in Fluids*, 4:619–640, 1984.
- [2] T. Tamura and K. Kuwahara. Direct finite difference computation of turbulent flow around a circular cylinder. *Proc. of International Symposium of Computational Fluid Dynamics, 1989*, 701–706, 1989.
- [3] M. Tabata and S. Fujima. Finite-element analysis of high Reynolds number flows past a circular cylinder. *Journal of Computational and Applied Mathematics*, 38:411–424, 1991.
- [4] S. Shirayama. Flow past a sphere: Topological transitions of the vorticity field. *AIAA Journal*, 30:349–358, 1992.
- [5] T. E. Tezduyar, S. Mittal, S. E. Ray, and R. Shih. Incompressible flow computations with stabilized bilinear and linear equal-order-interpolation velocity-pressure elements. *Computer Methods in Applied Mechanics and Engineering*, 95:221–242, 1992.
- [6] M. Tabata. Mixed and stabilized finite element approximations to axisymmetric flow problems. In S. Wagner et al., editors, *Computational Fluid Dynamics '94*, pages 176–180, John Wiley & Sons, Baffins Lane, Chichester, 1994.
- [7] M. Tabata. Finite element analysis of axisymmetric flow problems. To appear in *Proceedings of ICIAM 95*, Akademie Verlag, Berlin.
- [8] A. Mizukami. A mixed finite element method for boundary flux computation. *Computer Methods in Applied Mechanics and Engineering*, 57:239–243, 1986.
- [9] P. M. Gresho, R. L. Lee, R. L. Sani, M. K. Maslanik, and B. E. Eaton. The consistent Galerkin FEM for computing derived boundary quantities in thermal and/or fluids problems. *International Journal for Numerical Methods in Fluids*, 7:371–394, 1987.
- [10] T. J. R. Hughes, L. P. Franca, I. Harari, M. Mallet, F. Shakib, and T. E. Spelce. Finite element method for high-speed flows: Consistent calculation of boundary flux. In *AIAA 25th Aerospace Sciences Meeting, AIAA-87-0556*, 1987.
- [11] B. Mercier and G. Raugel. Résolution d'un problème aux limites dans un ouvert axisymétrique par éléments finis en  $r, z$  et série de Fourier en  $\theta$ . *R.A.I.R.O. Analyse numérique/Numerical Analysis*, 16:405–461, 1982.

- [12] K. Itakura. Doctor thesis, in preparation.
- [13] L. P. Franca, S. L. Frey, and T. J. R. Hughes. Stabilized finite element methods: I. Application to the advective-diffusive model. *Computer Methods in Applied Mechanics and Engineering*, 95:253–276, 1992.
- [14] L. P. Franca and S. L. Frey. Stabilized finite element methods: II. The incompressible Navier-Stokes equations. *Computer Methods in Applied Mechanics and Engineering*, 99:209–233, 1992.
- [15] H. Schlichting. *Boundary-Layer Theory*. McGraw-Hill, New York, 7th edition, 1979.